ALEPH 99-014
CONF 99-009
March 12, 1999
EPS-HEP 99 Abst# 5-621

PRELIMINARY

Measurement of the tau leptonic branching ratios at LEP I

ALEPH Collaboration

Contact person : Henri Videau (videau@poly.in2p3.fr)

Abstract

Using a sample of about 200000 produced τ-pair events collected by ALEPH from 1991 to 1995, the branching ratios of the tau lepton to electron and muon are measured. The results are : $\mathcal{B}_e = 17.783 \pm 0.072(\text{stat.}) \pm 0.032(\text{syst.})(\%)$ and $\mathcal{B}_\mu = 17.290 \pm 0.069(\text{stat.}) \pm 0.029(\text{syst.})(\%)$. These results allow to check the universality of the couplings in the leptonic charged current at the 3 per mille level.

1 Introduction

The measurement of the tau leptonic branching ratios allows to test the standard model in the lepton sector of the charged current, providing with the measurement of the tau lifetime a check of the universality of the charged current couplings to the three lepton families.

The full LEP I data sample collected by ALEPH is used in this measurement of the tau leptonic branching ratio. Two methods have been devised which corroborate these now very precise results.

The first one follows with some improvements the method described in [1]. This paper contains ALEPH leptonic branching ratio results for 1991 to 1993 data. It provides results for the samples collected during the remaining years of LEP I, 1994 and 1995. The second method is rather different and follows more closely the approach used in the tau polarisation analysis [2]. It analyses the full sample. The results are year by year and globally perfectly compatible.

The essentials of the first method are first recalled with a description of the improvements. Then the basics of the second are exposed. Finally the results are compared and combined to provide the best results.

2 The first method

2.1 Overview of the method

The analysis starts with the selection of $\tau\tau$ events with a large overall efficiency ($\varepsilon_{\tau\tau}^{sel} \sim 79\%$) and a small contamination from background processes (fraction $f_{\tau\tau}^{non-\tau} \sim 1.2\%$). The $\tau\tau$ selection efficiency is quite uniform over the different τ decay modes, in particular for the two leptonic channels ($\varepsilon_{\ell}^{sel} \sim 77\%$ for electrons, $\sim 80\%$ for muons). The non-τ background contamination in the lepton channels is small ($f_{\ell}^{non-\tau} \sim 2.0\%$ for electrons, $\sim 1.3\%$ for muons). Most of the inefficiency in the selection comes from the geometrical acceptance of $\sim 85\%$. Leptons are identified efficiently (with efficiencies $\varepsilon_{\ell ID} \sim 94\%$ for electrons, $\sim 93\%$ for muons) with a small contamination from hadronic τ decays ($f_{h\to\ell}^{\tau} \sim 0.8\%$ for electrons, $\sim 1.1\%$ for muons). The branching ratios are obtained through the expression

$$\mathcal{B}_{\ell} = \frac{N_{\ell} - N_{\ell}^{non-\tau}}{(1 + f_{h\to\ell}^{\tau}) \cdot 2 \cdot N_{\tau\tau}(1 - f_{\tau\tau}^{non-\tau})} \cdot \frac{\varepsilon_{\tau\tau}^{sel}}{\varepsilon_{\ell}^{sel}} \cdot \frac{1}{\varepsilon_{\ell ID}} \ , \tag{1}$$

where N_{ℓ} is the observed number of leptons, either electrons or muons.

In order to achieve systematic uncertainties at the level of a few 10^{-3}, the prevaluations of efficiencies and misidentifications from the simulation are corrected systematically with detailed comparisons with the data. The major non-τ background contributions are determined directly on the final data sample using only the shape of the distributions of the discriminating variables from the simulation.

The data taken in 91-93 have already been analyzed and published using this method [1]. It is the purpose of the present work to update the results using the remaining data registered in 94-95. The philosophy remains the same with some simplification of the selection procedure, and improvements in the determination of the non-τ backgrounds and of the selection efficiencies.

The determination of the systematic uncertainties is described in the relevant sections. Smaller systematic effects, such as the effect of hadronic branching ratios and τ polarisation used in the $\tau\tau$ event generator KORAL07 are taken from the previous analysis [1].

2.2 Event selection and efficiencies

The preselection of $\tau\tau$ events (cuts 1 to 11 in table 1), follows exactly the procedure developed in the previous analysis [1], with only a small change concerning the cuts 7 and 8, to veto hadronic Z decays, already used in the analysis of τ hadronic branching ratios [3]. Contrary to Ref. [1], the further selection step is reduced considerably, keeping only the cosmic ray veto and only one cut to reduce the remaining Bhabha background, asking the total energy measured on the ECAL wire planes to be less than 1.8 E_{beam}. This last cut removes Bhabha events where the observed ECAL pad energy is reduced because of inefficient or dead channels. This simpler selection is easier to handle for the determination of the efficiencies. While the corresponding non-τ background is slightly higher, this does not cause any problem as its level is directly measured on the data.

Table 1: List of cuts used in $\tau\tau$ events selection.

Index	cut
1	$2 \leq n_{ch} \leq 8$
2	$min(n_{ch,1}, n_{ch,2}) \geq 1$
3	$-0.9 < \cos\theta^* < 0.9$
4	$ACOL > 160°$
5	$E_{tot} > 0.35 \cdot E_{beam}$ or $\lvert\Delta p_t\rvert > 0.066 \cdot E_{beam}$
6	at least 1 good track has $\lvert d_0\rvert < 1$ cm and $\lvert z_0\rvert < 5$ cm
7	$\tau - like$: $n_{ch,i} = 1$ and $m_i < 0.8$ GeV
8	if not $\tau - like$: $n_{obj,1} \cdot n_{obj,2} < 40$ and $\theta_1^{open} + \theta_2^{open} < 0.25$ rad.
9	$E_1^{ldg} + E_2^{ldg} < 1.6 \cdot E_{beam}$
10	$Bhabha - like$ (all the charged tracks are electrons): $E_{tot}/E_{beam} < 1.6$ when $Min_{DG} > 6$ cm or $E_{tot}/E_{beam} < 1.4$ when $Min_{DG} < 6$ cm.
11	$Dimu - like$ (both leading tracks are muons, or one is muon and energy in opposite hemisphere greater than $0.9 \cdot E_{beam}$): $E_{tot}/E_{beam} < 1.8$.
12	$E_{tot,ECAL}^{wire} > 1.8 \cdot E_{beam}$
13	*cosmic rays veto*

The determination of the final selection efficiencies proceeds by the detailed comparison of the efficiency of each cut in data and in the simulation. For every cut used, unbiased tau decays are tagged in the selected data by judiciously choosing the opposite hemisphere not to be contaminated by non-τ background and to insure that events of this type were not affected by the cut under study. Fake $\tau\tau$ are constructed by forming combinations in the sample of unbiased hemispheres. The same procedure is applied to the simulation. The ratio data/MC of the cut efficiencies is measured and this correction is applied to the MC efficiency which correctly takes into account the small correlations between opposite hemispheres which were lost in the previous step. This "break-mix" procedure was already successfully used in the measurement of the $\tau\tau$ cross section [4] and in the previous branching ratio analysis [1, 3], but only for the cut against hadronic Z decays where the detailed simulation was more questionable. Tables 2, 3 and 4 give the results of this procedure for $\tau\tau$ events, and electron and muon decays for 94 data. Similar results are obtained for 95 data.

2.3 Particle Identification

The definition of the electron and muon hemispheres follows exactly that used in the published analysis [1]. A single track is required to avoid identification and reconstruction problems from the presence

Table 2: Selection Efficiencies for $\tau\tau$ events(%), 94 data.

Cut	Data (BM)	Monte Carlo (BM)	Monte Carlo
1–4	–	—	82.525 ± 0.056
5	98.751 ± 0.037	98.737 ± 0.017	98.839 ± 0.017
6	99.997 ± 0.001	99.998 ± 0.000	99.996 ± 0.001
7 or 8	98.021 ± 0.049	98.262 ± 0.025	98.324 ± 0.021
9	99.518 ± 0.015	99.569 ± 0.007	99.436 ± 0.012
10	99.388 ± 0.035	99.293 ± 0.015	99.212 ± 0.015
11	99.620 ± 0.026	99.703 ± 0.009	99.666 ± 0.010
5–11	95.374 ± 0.074	95.633 ± 0.035	95.548 ± 0.034
12			99.980 ± 0.002
13			99.999 ± 0.000
12–13			99.980 ± 0.002
1–13	78.621 ± 0.090	—	78.835 ± 0.060

Table 3: Selection Efficiencies for $\tau \to \nu_\tau e \bar{\nu_e}$ decays (%), 94 data.

Cut	Data (BM)	Monte Carlo (BM)	Monte Carlo
1–4	–	—	81.105 ± 0.097
5	97.318 ± 0.085	97.185 ± 0.060	97.434 ± 0.043
6	99.996 ± 0.001	99.998 ± 0.001	99.996 ± 0.002
7 or 8	99.879 ± 0.017	99.920 ± 0.012	99.704 ± 0.015
9	99.577 ± 0.019	99.708 ± 0.016	99.686 ± 0.016
10	98.846 ± 0.073	98.720 ± 0.050	98.629 ± 0.032
11	99.969 ± 0.007	99.994 ± 0.001	99.979 ± 0.004
5–11	95.639 ± 0.112	95.577 ± 0.079	95.490 ± 0.057
12			99.991 ± 0.003
13			100.000 ± 0.000
12–13			99.991 ± 0.003
1–13	77.490 ± 0.152	—	77.440 ± 0.103

Table 4: Selection Efficiencies for $\tau \to \nu_\tau \mu \bar{\nu_\mu}$ decays (%), 94 data.

Cut	Data (BM)	Monte Carlo (BM)	Monte Carlo
1–4	–	—	83.209 ± 0.094
5	97.482 ± 0.072	97.505 ± 0.062	97.348 ± 0.044
6	100.000 ± 0.000	100.000 ± 0.000	100.000 ± 0.000
7 or 8	99.929 ± 0.009	99.931 ± 0.011	99.792 ± 0.013
9	99.499 ± 0.021	99.567 ± 0.022	99.569 ± 0.018
10	99.976 ± 0.008	99.978 ± 0.007	99.971 ± 0.005
11	99.232 ± 0.054	99.301 ± 0.031	99.345 ± 0.023
5–11	96.157 ± 0.091	96.317 ± 0.073	96.065 ± 0.054
12			99.984 ± 0.004
13			99.996 ± 0.002
12–13			99.980 ± 0.004
1–13	79.786 ± 0.140	—	79.919 ± 0.101

of converted photons. Particles identified as leptons are not kept in the sample if their hemisphere shows some "hadronic" activity, signaled by a π^0 reconstruction or a total hadronic mass in the expected range.

Then the particle identification is performed using a likelihood method to incorporate the information from the relevant detectors. In this way, each charged particle is assigned a set of probabilities from which a particle type is chosen. The particle identification is based on the following information: dE/dx in the TPC; longitudinal and transverse shower profile in ECAL near the extrapolated track; energy and average shower width in HCAL, together with the number of fired planes in the last 10 planes of HCAL and hits in the muon chambers.

The performance of this identification has been studied in detail using samples of Bhabhas, μ-pairs, $\gamma\gamma$-induced lepton pairs and hadrons from π^0-tagged τ decays over the full angular and momentum range. The detailed procedure is given in Ref. [1].

The measurement of the electron and muon ID efficiencies are given in Figs. 1 and 2. The prediction for the simulation is also given for the same data samples. The ratio data/MC as a function of momentum is then applied to the MC corresponding efficiencies for the $\tau\tau$ sample. This procedure takes care of the slightly different environment for a given particle between the various samples.

Similarly, hadronic τ decays tagged with a reconstructed π^0 are used to determine the hadron misidentification probabilities into electron or muon. The results are given in Figs. 3 and 4. Significant differences are observed between data and simulation, as in previous years, emphasizing the necessity of measuring directly these quantities on the data. The measured misidentification probabilities are then folded with the hadron momentum distribution in τ decays to obtain the final hadron contamination in each lepton sample, taking into account the hadronic veto discussed above.

2.4 Non-τ background

Here a new method is developed to directly measure in the final data samples the contributions of the major non-τ backgrounds: Bhabhas, $\mu^+\mu^-$ pairs, and $\gamma\gamma \to e^+e^-, \mu^+\mu^-$ events. The procedure does not require an absolute normalization from the simulation of these channels, only a qualitative description of the distribution of the discriminating variables. The basic idea is to apply cuts on the data in order to reduce as much as possible the $\tau\tau$ population while keeping a high efficiency for the background source under study.

For Bhabha background, different event topologies are considered in turn. For *e-e* and *e-crack* topologies, the acoplanarity angle is required to be larger than 179° or the acolinearity angle should be less than 175° with the difference of transverse energies being less than 3 GeV. The corresponding Bhabha efficiency (for the final sample) is 88% as determined from the simulation using UNIBAB. The angular distribution of the restricted sample is then fitted to $\tau\tau$ and Bhabha components (also including a small contribution from the other non-τ backgrounds) from the simulation. Therefore, the Bhabha MC input is only used to determine the (large) selection efficiency and the $\cos\theta$ shape inside the final sample, not relying on any determination of the absolute MC normalization. The derived Bhabha contribution has a statistical uncertainty which is assigned as a systematic error. Several combinations of variables have been tried, showing a good stability of the result within its error. Fig. 5 illustrates the determination for the *e-e* topology. For the more numerous *e-hadron* sample, the same cuts are used, but they have to be supplemented by an additional requirement to suppress true hadrons as compared to electrons misidentified as hadrons: this is achieved by restricting opposite hadrons to have an electron ID probability larger than 0.01 (most of the true hadrons are below this value).

A similar technique is used to estimate the μ-pair background. Fig. 6 shows the corresponding plots for the μ-μ topology, requiring an acoplanarity angle larger than 178° (90% efficiency for $\mu\mu$ events in the final sample). Here, the fitted distribution is that of the calculated photon energy along the beam for

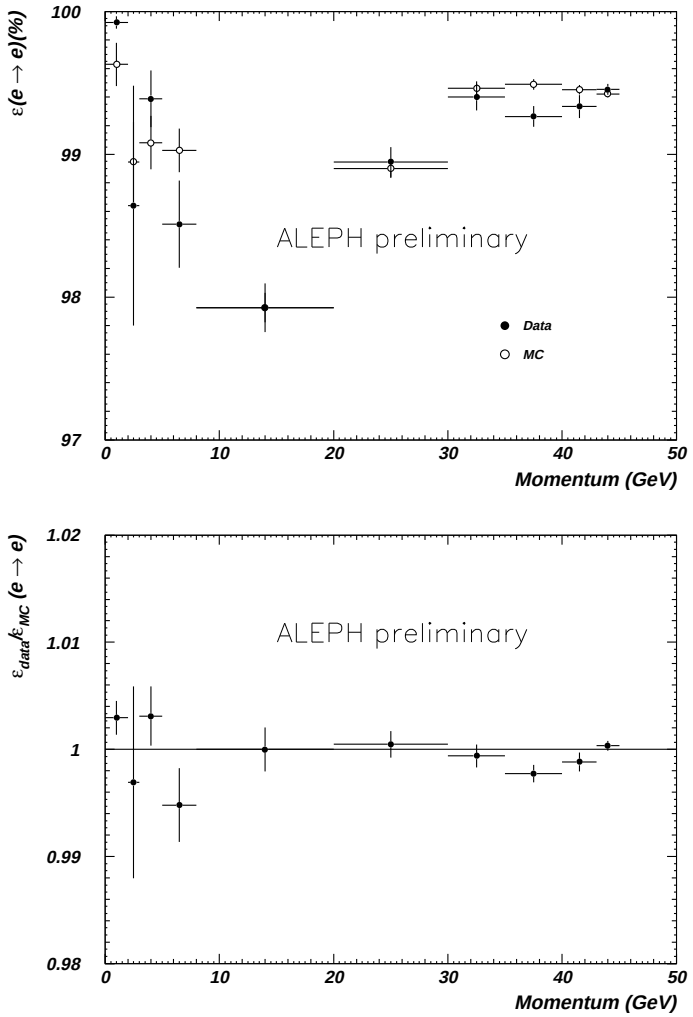

Figure 1: Particle identification efficiencies for electrons as a function of momentum, determined from special samples (see text). The top plot gives the absolute efficiencies for data and simulation, while their ratio is displayed below. The efficiencies are determined excluding tracks going through ECAL cracks between modules.

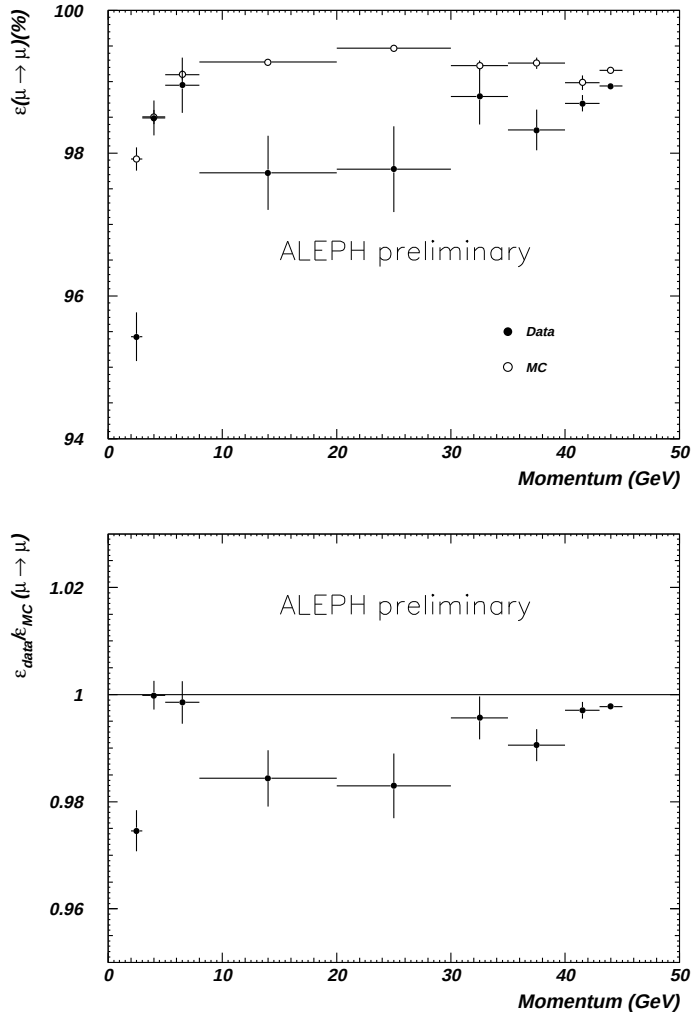

Figure 2: Particle identification efficiencies for muons as a function of momentum, determined from special samples (see text). The top plot gives the absolute efficiencies for data and simulation, while their ratio is displayed below.

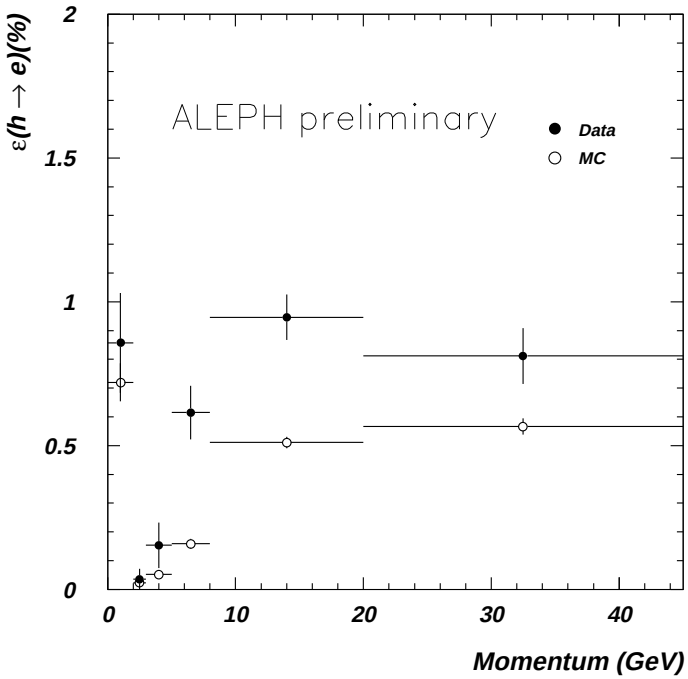

Figure 3: Misidentification probabilities into electron (94+95 data) for hadrons as a function of momentum, determined from the hadron test sample (see text). Data and simulation results are given.

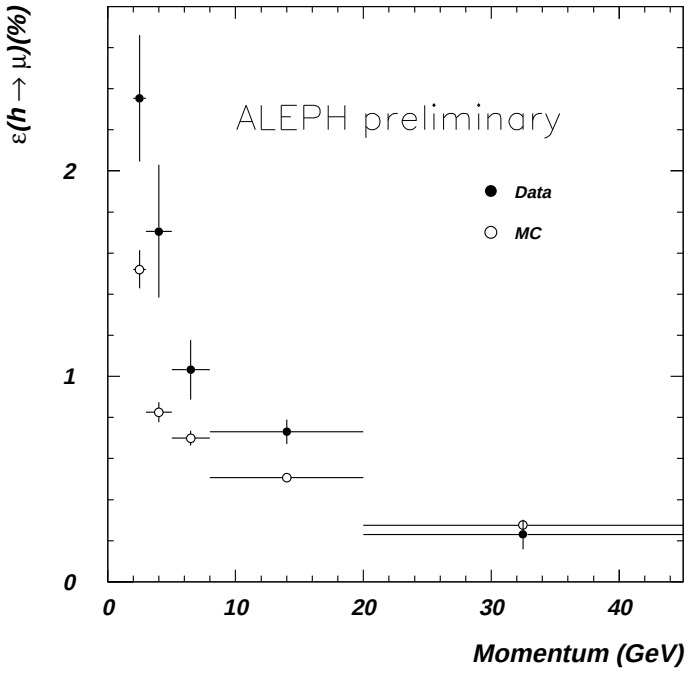

Figure 4: Misidentification probabilities into muon (94+95 data) for hadrons as a function of momentum, determined from the hadron test sample (see text). Data and simulation results are given.

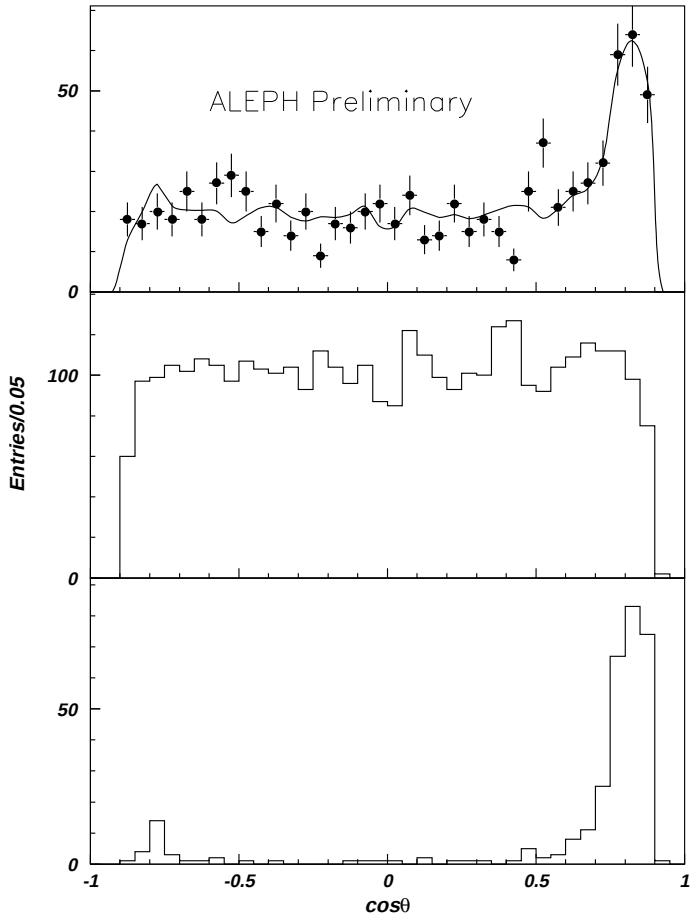

Figure 5: Determination of the remaining Bhabha contribution in the final e-e sample for 94/95 data(see text). The plot on the top shows the data (black dots) and the result of the fit (line) of the 2 contributions, the tau tau MC (middle plot) and the Bhabha (lower plot)

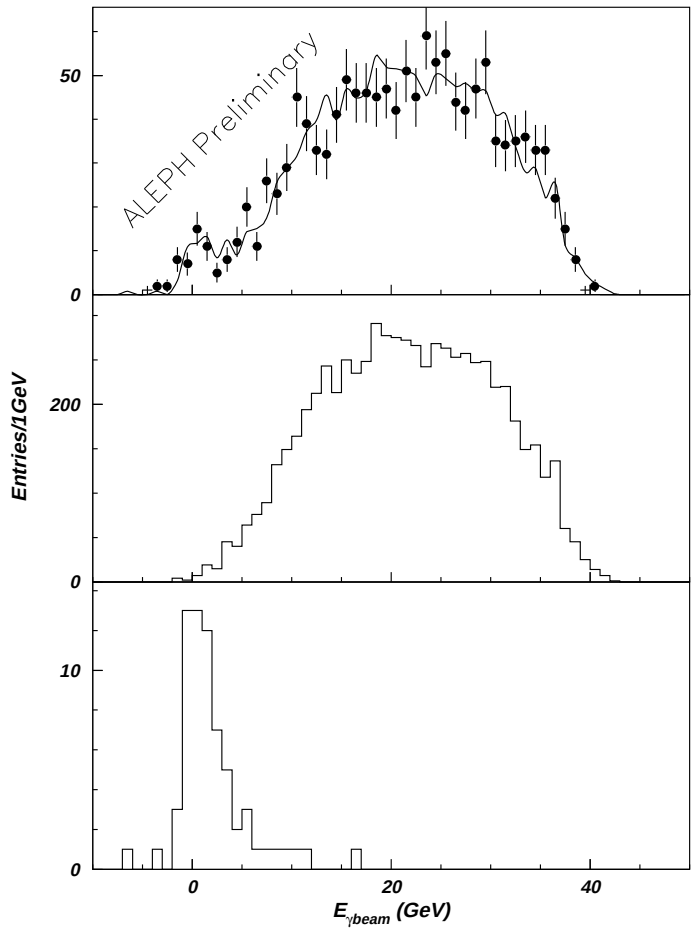

Figure 6: Determination of the remaining $\mu\mu$ contribution in the final μ-μ sample for 94/95 data (see text). The plot on the top shows the data (black dots) and the result of the fit (line) of the 2 contributions, the tau tau MC (middle plot) and the Z$\rightarrow \mu\mu$ MC (lower plot).

a postulated $\mu\mu\gamma\gamma_{beam}$ kinematics to take the most general case compatible with the only information on the two muons. The $\mu\mu$ background signal is clearly seen for small energies.

The remaining background from $\gamma\gamma \to \mu\mu$ is easily found in the μ-μ topology after requiring the acolinearity angle to be smaller than 170° leading to an efficiency of 57%. The distribution of the acoplanarity angle shows a distinct signal for the background, as seen in Fig. 7.

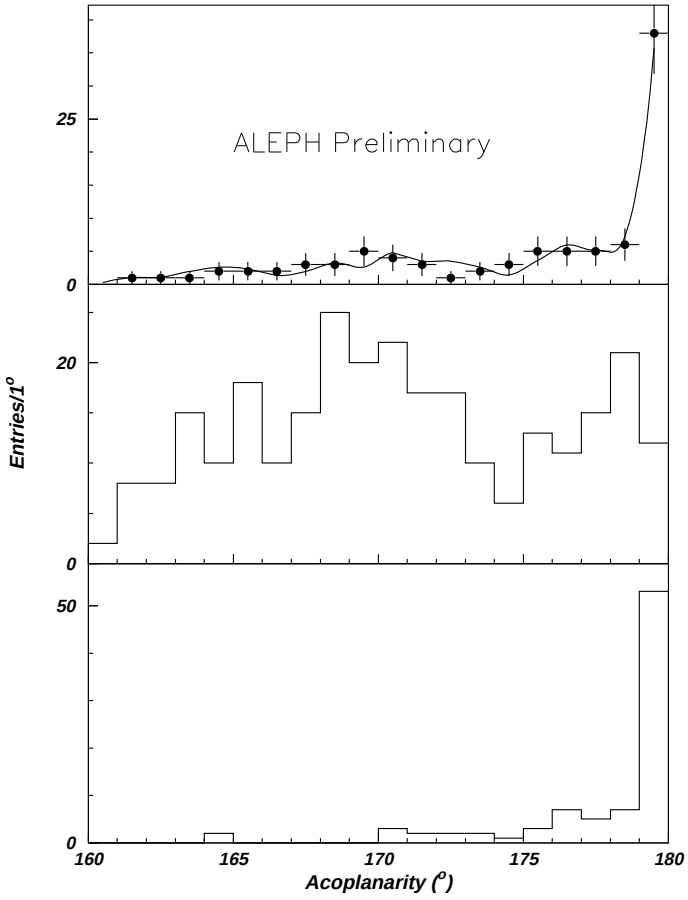

Figure 7: Determination of the remaining $\gamma\gamma \to \mu\mu$ contribution in the final μ-μ sample for 94/95 data (see text). The plot on the top shows the data (black dots) and the result of the fit (line) of the 2 contributions, the tau tau MC (middle plot) and the $\gamma\gamma \to \mu\mu$ MC (lower plot).

The same procedure is applied for $\gamma\gamma \to ee$, but additional cuts (for example requiring the total event energy to be less than 35 GeV) must be applied to decrease the Bhabha contribution.

Cosmic ray background is determined to be very small after the additional cuts [1]. All other contributions are small in the leptonic channels and are safely estimated with the proper Monte Carlo generators. The contamination from hadronic Z decays is also estimated from the Lund generator. Tests were previously made to ascertain the reliability of the prediction for the rate of surviving low multiplicity events by comparing with data [3].

The non-τ background contributions are given in Tables 5 and 6, separately for the selected $\tau\tau$, electron and muon samples.

Table 5: Non-τ backgrounds in 94 τ samples.

Source	Evts in $\tau\tau$	Evts in e sample	Evts in μ sample
$e^+e^- \to e^+e^-(\gamma)$	238.9 ± 26.0	348.0 ± 38.4	0.0 ± 0.0
$e^+e^- \to \mu^+\mu^-(\gamma)$	85.6 ± 12.6	0.0 ± 0.0	129.0 ± 19.5
Cosmic Ray	13.0 ± 3.6	0.0 ± 0.0	2.2 ± 1.5
$\gamma\gamma \to e^+e^-$	34.0 ± 12.0	55.0 ± 20.6	0.0 ± 0.0
$\gamma\gamma \to \mu^+\mu^-$	77.1 ± 14.8	3.5 ± 1.4	143.7 ± 26.7
$\gamma\gamma \to \tau^+\tau^-$	25.0 ± 3.0	9.0 ± 2.0	5.6 ± 1.2
$\gamma\gamma \to q\bar{q}$	13.0 ± 6.0	0.0 ± 0.0	0.0 ± 0.0
$Z^0 \to q\bar{q}$	226.0 ± 68.0	2.5 ± 0.8	1.6 ± 0.5
$e^+e^- \to l^+l^-f\bar{f}$	68.0 ± 2.0	35.0 ± 1.0	14.0 ± 1.0
total	780.6 ± 76.7	453.0 ± 43.7	296.1 ± 33.1

Table 6: Non-τ backgrounds in 95 τ samples.

Source	Evts in $\tau\tau$	Evts in e sample	Evts in μ sample
$e^+e^- \to e^+e^-(\gamma)$	140.9 ± 18.8	208.5 ± 28.9	0.0 ± 0.0
$e^+e^- \to \mu^+\mu^-(\gamma)$	37.6 ± 7.8	0.0 ± 0.0	53.3 ± 12.3
Cosmic Ray	6.0 ± 2.4	0.0 ± 0.0	1.1 ± 1.0
$\gamma\gamma \to e^+e^-$	22.8 ± 8.4	42.0 ± 16.4	0.0 ± 0.0
$\gamma\gamma \to \mu^+\mu^-$	32.7 ± 9.2	1.5 ± 0.7	61.0 ± 16.6
$\gamma\gamma \to \tau^+\tau^-$	18.0 ± 2.0	6.0 ± 1.0	3.9 ± 0.9
$\gamma\gamma \to q\bar{q}$	6.0 ± 3.0	0.0 ± 0.0	0.0 ± 0.0
$Z^0 \to q\bar{q}$	108.0 ± 32.0	1.2 ± 0.4	0.8 ± 0.2
$e^+e^- \to l^+l^-f\bar{f}$	37.0 ± 1.0	19.0 ± 1.0	7.6 ± 0.3
total	409.0 ± 40.2	278.2 ± 33.3	127.7 ± 20.7

2.5 Results

The momentum spectra of the final electron and muon samples are shown in Figs. 8 and 9. Good agreement is observed with the Monte Carlo prediction within the quoted uncertainties, taking into account the non-τ background sources.

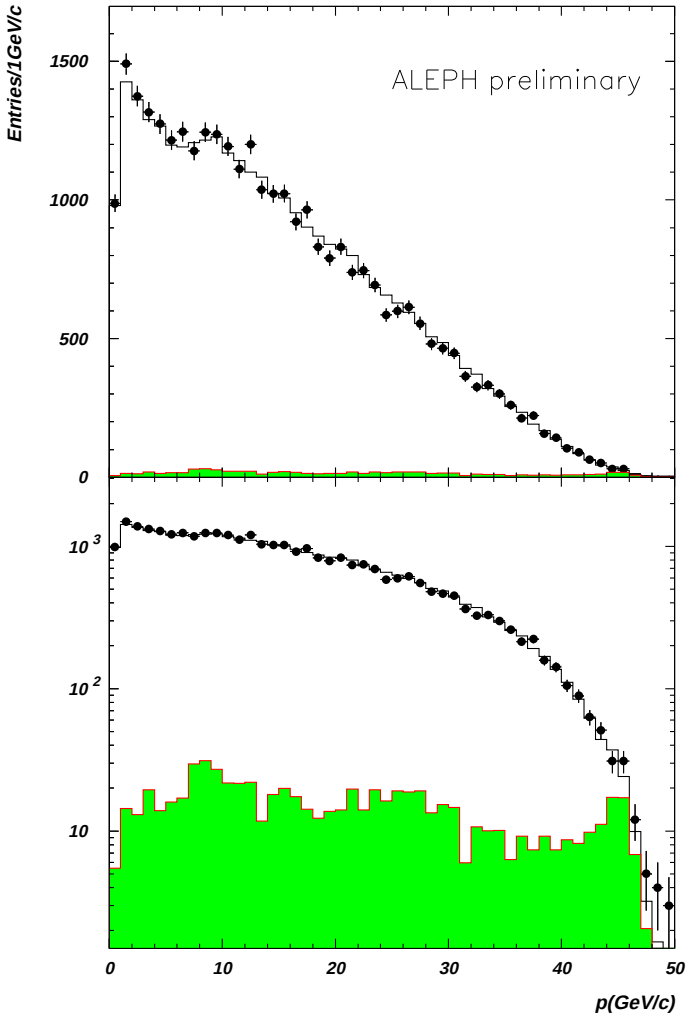

Figure 8: Momentum spectrum for electrons in 94/95 data. The Monte Carlo prediction is given by the histogram, with the non-τ background shown in shaded histogram.

The summary on the statistical and the different systematic uncertainties appears in Table 7.

The final measured quantities appearing in Eq. (1) and the branching ratio values are given in Tables 8 and 9. They are in excellent agreement with the published 91-93 results from which they are uncorrelated, except for a few systematic uncertainties which are below the 10^{-3} level.

The combined 94-95 results are

$$\begin{aligned} \mathcal{B}(\tau^- \to \nu_\tau e^- \bar{\nu}_e) &= (17.774 \pm 0.092 \pm 0.054)\% \ , \\ \mathcal{B}(\tau^- \to \nu_\tau \mu^- \bar{\nu}_\mu) &= (17.270 \pm 0.090 \pm 0.050)\% \ . \end{aligned}$$

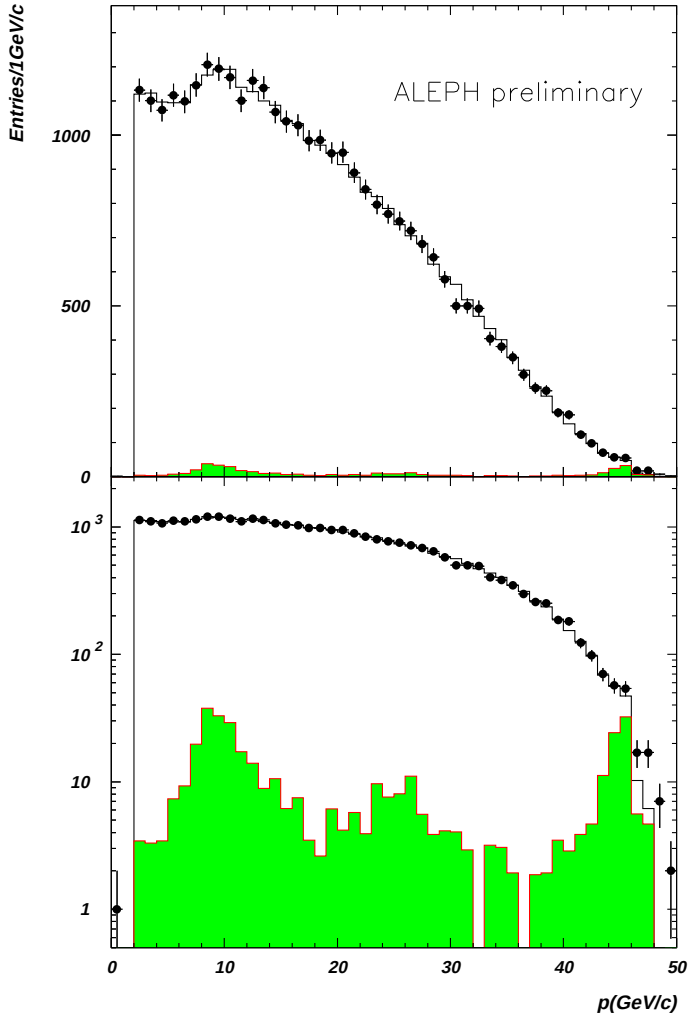

Figure 9: Momentum spectrum for muons in 94/95 data. The Monte Carlo prediction is given by the histogram, with the non-τ background shown in shaded histogram.

Table 7: Summary of Error (10^{-3}).

Source	$\mathcal{B}_e$ (94)	$\mathcal{B}_\mu$ (94)	$\mathcal{B}_e$ (95)	$\mathcal{B}_\mu$ (95)
Statistics (Data)	6.2	6.3	9.5	9.4
Statistics (MC)	1.3	1.3	1.8	1.7
$\varepsilon_{\tau\tau}$	1.1	1.1	1.9	1.9
$N_\tau^{non-\tau}$	1.2	1.2	1.4	1.4
ε_ℓ	1.4	1.2	2.6	2.6
$N_\ell^{non-\tau}$	2.0	1.5	3.5	2.2
$\varepsilon_{\ell ID}$	1.3	1.7	1.9	2.9
$\varepsilon_{h\to\ell}$	0.6	0.7	0.9	1.3
single track	0.7	0.4	0.7	0.4
hadron BR	0.4	0.4	0.4	0.4
τ polarisation	0.2	0.4	0.2	0.4
total systematics	3.6	3.4	5.7	5.5

Table 8: Branching Ratios (1994).

	n^{obs}	$n^{non-\tau}$	$\varepsilon_{sel}(\%)$	$f^{\tau}_{h\to\ell}(\%)$	$\varepsilon_{\ell ID}(\%)$	Branching Ratio (%)
$\tau\tau$	66377	781 ± 77	78.62 ± 0.09	–	–	–
e	22366	453 ± 44	77.49 ± 0.15	0.78 ± 0.06	93.97 ± 0.12	$17.90 \pm 0.11 \pm 0.06$
μ	21925	296 ± 33	79.79 ± 0.14	1.12 ± 0.07	93.06 ± 0.15	$17.26 \pm 0.11 \pm 0.06$

Table 9: Branching Ratios (1995).

	n^{obs}	$n^{non-\tau}$	$\varepsilon_{sel}(\%)$	$f^{\tau}_{h\to\ell}(\%)$	$\varepsilon_{\ell ID}(\%)$	Branching Ratio (%)
$\tau\tau$	29450	409 ± 40	78.72 ± 0.15	–	–	–
e	9759	278 ± 33	77.95 ± 0.24	0.77 ± 0.09	93.49 ± 0.18	$17.50 \pm 0.17 \pm 0.10$
μ	9638	128 ± 21	79.79 ± 0.25	0.94 ± 0.13	92.75 ± 0.27	$17.29 \pm 0.16 \pm 0.10$

Combining these results with those of published 91-93 data, the results for 91-95 ALEPH data are:

$$\begin{aligned} \mathcal{B}(\tau^- \to \nu_\tau e^- \bar{\nu}_e) &= (17.780 \pm 0.073 \pm 0.040)\% \ , \\ \mathcal{B}(\tau^- \to \nu_\tau \mu^- \bar{\nu}_\mu) &= (17.287 \pm 0.070 \pm 0.035)\% \ . \end{aligned}$$

3 The second method

The second method relies on the tools developed for the tau polarisation measurement [2] . It identifies and selects directly single tau hemispheres without prior selection of tau pair events. The number of tau pairs is derived using the cross section measurement performed by ALEPH [5].

The error on the luminosity and $\tau^+\tau^-$ cross section is the main uncertainty on the branching ratio measurement. However, this error cancels when the ratio of electron to muon branching ratios is used to test the universality of the charged current in the standard model.
The calibration of the momentum and the ECAL response performed for the tau polarisation analysis [2] have been used for this analysis.

To compute the branching ratio $\mathcal{B}_\ell$, the following expression is used.

$$\mathcal{B}_\ell \ = \ (\mathrm{N}_\ell - \mathrm{N}_\ell^{non-\tau})\,(1 - f^{\tau}_{h\to\ell})\,\frac{1.}{\varepsilon_\ell^{sel.} N\tau} \qquad (2)$$

where

N_ℓ is the number of leptons ℓ selected,
$\mathrm{N}_\ell^{non-\tau}$ is the estimated non-tau background,
$f^{\tau}_{h\to\ell}$ is the fraction of tau hadronic background,
$\varepsilon_\ell^{sel.}$ is the overall selection efficiency, including lepton identification ,
$\mathrm{N}\tau$ is the number of taus in the data.

3.1 Particle Identification

The charged track particle identification (called hereafter " **PID** ") is the one used for the measurement of the charge forward-backward asymmetry of the lepton [5] and the tau polarisation measurement [2].

The **PID** efficiency is measured on data and is found to be correctly modelled by the Monte Carlo within 0.2%. In order to have an unbiased average measurement between years of data taking, the efficiency is tested year by year. Therefore, the branching ratio is corrected and the systematic error estimated for each year independently.

The rate of hadron misidentification is tested using a "hadronic tau decay" sample. This sample is selected using the reconstructed π^0, and the hemisphere mass, which must lie in the ρ/a_1 region. Figure 10 shows the rate of h$\rightarrow$ e and h$\rightarrow$ μ for this selected 1991-1995 data sample and the equivalent in the $\tau^+\tau^-$ Monte Carlo. This is just an illustration, like the test of the **PID** efficiencies, the rate of misidentification being tested for each year independently, and the branching ratio corrected year by year. The rate of muon/electron misidentification is very small, leading to a cross talk between τ decays into muon and electron smaller than 2.5 10^{-4}.

The photons are reconstructed using the standard ALEPH reconstruction algorithm [6] followed by a fake photon estimation described in [2]. The efficiency for genuine photons as well as the rate of fake photons which feed through are described in the same reference.

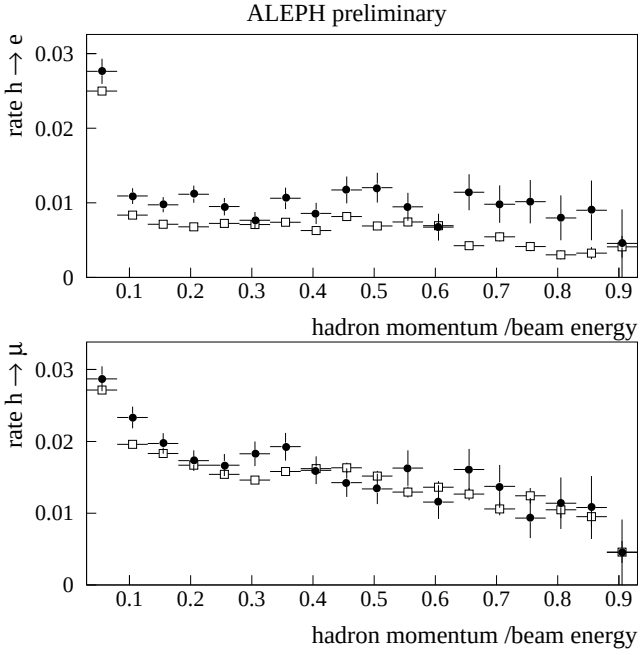

Figure 10: The rate of misidentification h$\rightarrow$ e on the top and h$\rightarrow$ μ below. The black dots are the 1991-1995 data and the empty squares are the $\tau^+\tau^-$ Monte Carlo.

3.2 The pre-selection

For both channels, the pre-selection is the following:
- the event is in the standard loose lepton pairs preselection ALEPH sample [5],
- after subtraction of the γ conversions, there is only one track coming from the vertex region ($|do|$ <2 cm and $|Zo|$ <5 cm), where do is the closest appraoch to the beam direction and Zo is the z position of

the track along the beam line,
- $|cos\theta^*| < 0.9$, where θ^* is the scattering angle in the $\tau\tau$ rest frame,
- $\cos\theta_{acol.} < -0.9$, where $\theta_{acol.}$ is the acollinearity angle computed from the charged tracks,
- the 2 hemispheres have consistent charges (no same sign, charge zero accepted as soon as the opposite hemisphere has a charge ± 1).

This pre-selection has an efficiency of 81.4% for the electron channel and 83.2% for the muon channel.

3.3 The $\tau \to e\nu_e\nu_\tau$ channel

The $\tau \to e\nu_e\nu_\tau$ hemisphere sample is selected as :
• events in the pre-selected sample
then the hadronic tau decays are rejected
• the track does not extrapolate to an ECAL crack if the momentum is larger than $0.2E_{beam}$ or if there is no dE/dX information avalaible,
• the track is identified as an electron,
• the hadronic veto, which rejects hemisphere with reconstructed π^0
and finally, the non-tau background is rejected
• Bhabha rejection, based on energy and a likelihood estimator discrimating Bhabha from $\tau^+\tau^-$ events as already used in reference [2]
• 2-photon rejection, based on the kinematics of the event.

The selection efficiency is about 69%, with a tau contamination of 1% and a non-tau contamination of 1.5%. To illustrate the selection, figure 11 shows for the data and Monte Carlo the distribution of the sum of the 2 estimator responses (on per hemipshere) for the Bhabha/$\tau^+\tau^-$ estimator, and figure 12 shows the total ECAL energy distribution before the last cut gainst the Bhabha background.

A total of 48882 hemispheres are selected.
The following systematic errors have been studied, the non-tau background, the tau background, the selection efficiency and the number of tau. This last error represents about 90% of the total systematic uncertainty. All the systematics are summarized in the table 10.

3.4 The $\tau \to \mu\nu_\mu\nu_\tau$ channel

The $\tau \to \mu\nu_\mu\nu_\tau$ hemisphere sample is selected as :
• events in the pre-selected sample,
then , the hadronic tau decays are rejected by
• the track momentum larger than 1.3 GeV,
• the track identified as an muon,
• the hadronic veto, which rejects hemisphere with reconstructed π^0
and finally, the non-tau background is rejected by
• the Z$\to \mu^+\mu^-$ rejection based on an estimator discrimating Z$\to \mu^+\mu^-$ from Z$\to \tau^+\tau^-$ events, as already used in reference [2]
• the 2-photon rejection, based on the kinematic of the event,
• the cosmic rejection, based on the track properties such as the closest approach from the vertex.

The selection efficiency is about 75%, with a tau contamination of 0.8% and a non-tau contamination of 0.4%. To illustrate the selection, figure 13 shows for the data and Monte Carlo the distribution of the sum of the 2 estimator responses (one per hemipshere) for the $Z \to \mu^+\mu^-/\tau^+\tau^-$ estimator.

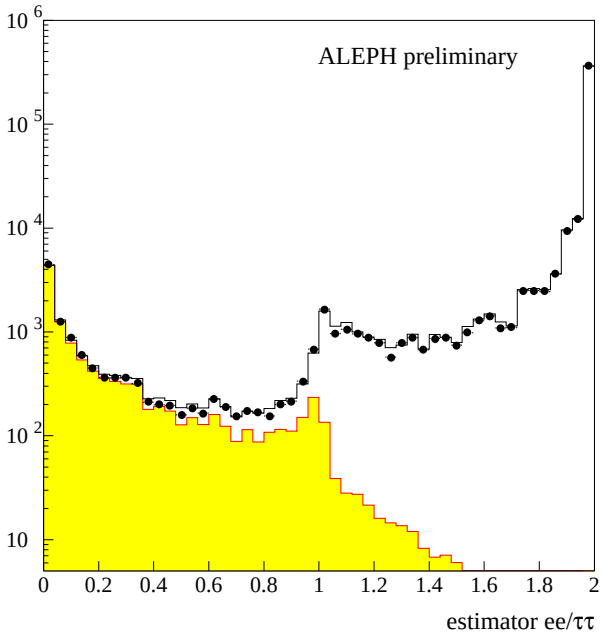

Figure 11: The distribution of the sum of the two estimators Bhabha/$\tau^+\tau^-$ for e^+e^- final state. The black dots are the data, the histogram is the $\tau^+\tau^-$ and UNIBAB MC prediction, and the dashed area shows the contribution of the $\tau^+\tau^-$ Monte Carlo.

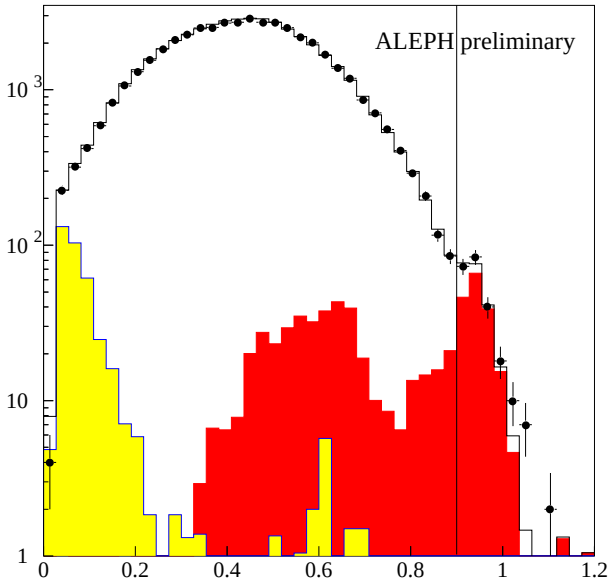

Figure 12: The distribution of the sum of the ECAL wires energy normalised to the center-of-mass energy, before the cut on the energy. The black dots are the data, the line histogram is the sum of all contribution, $\tau^+\tau^-$ KORALZ, $\gamma\gamma \to e^+e^-$ and $\gamma\gamma \to \tau^+\tau^-$ from PHOT02 and UNIBAB for Bhabha. All the non-tau backgrounds, shown by the grey histograms, are normalised using the methods described in the text. The vertical line shows the position of the cut.

A total of 50782 hemispheres are selected.
The following systematic errors have been studied, the non-tau background, the tau background, the selection efficiency and the numbers of tau. This last error represents about 90% of the total systematic uncertainty. All the systematics are summarized in the table 11.

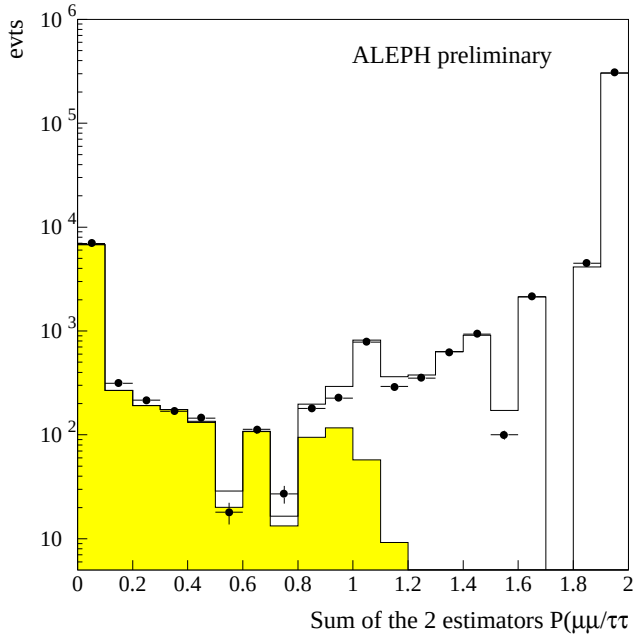

Figure 13: The distribution of the sum of the two estimators $P_{(Z\to\mu^+\mu^-)/(Z\to\tau\tau)}$ for $\mu^+\,\mu^-$ final state. The black dots are the data, the histogram is the $\tau^+\,\tau^-$ and $\mu^+\,\mu^-$ MC prediction, and the dashed area shows the contribution of the $\tau^+\,\tau^-$ Monte Carlo.

sources	1991	1992	1993	1994	1995
electron PID	0.008	0.006	0.005	0.0036	0.0057
Hadron misid.	0.021	0.015	0.015	0.0086	0.022
Bhabha back.	0.015	0.012	0.011	0.006	0.013
2-photon back.	0.043	0.050	0.052	0.028	0.033
stat. MC	0.036	0.030	0.038	0.032	0.034
sel. effic.†	0.018	0.018	0.018	0.018	0.030
sub-total	0.064	0.064	0.070	0.047	0.062
Number of tau	0.083	0.068	0.058	0.086	0.051
total	0.105	0.094	0.090	0.098	0.080

Table 10: The systematics on the tau to electron branching ratio (%). † this line is correlated between years of data taking, except 1995 .

3.5 Non-tau background

Each non-tau background is estimated from the corresponding Monte Carlo, UNIBAB [7] for the Bhabha, KORALZ for $\mu^+\,\mu^-$ [8], PHOT02 [9] for the 2-photon processes and FERMISV [12] for the $\ell\ell V$ processes.

To be insensitive to the absolute prediction of the non-tau processes, the non-tau background Monte Carlo is normalised to the excess in the data versus the $\tau^+\,\tau^-$ Monte Carlo, in the distribution of a

sources	1991	1992	1993	1994	1995
muon PID	0.031	0.020	0.012	0.004	0.083
Hadron misid.	0.014	0.017	0.017	0.006	0.050
Z$\rightarrow\mu^+\mu^-$ back.	0.013	0.006	0.001	0.001	0.018
2-photon back.	0.010	0.015	0.016	0.009	0.014
Cosmic	0.005	0.003	0.008	0.001	0.003
stat. MC	0.046	0.034	0.028	0.025	0.027
sel. effic.†	0.012	0.012	0.012	0.012	0.012
sub-total	0.062	0.047	0.041	0.030	0.104
Number of tau	0.082	0.066	0.053	0.083	0.051
total	0.103	0.081	0.067	0.088	0.115

Table 11: The systematics on the muon branching ratio (%). † this line is correlated between years of data taking.

variable separating the non-tau process from the $\tau^+\tau^-$. This variable is the likelihood estimator for the Bhabha and the Z$\rightarrow\mu^+\mu^-$ background, while the case of the cosmic background is treated apart. Likelihood estimators have been built to separate the $\tau^+\tau^-$ events from the Bhabha, ($P_{(e^+e^-\rightarrow e^+e^-)/(Z\rightarrow\tau\tau)}$), from the Z$\rightarrow\ \mu^+\mu^-$ ($P_{(Z\rightarrow\mu^+\mu^-)/(Z\rightarrow\tau\tau)}$) and from the Z hadronic decays ($P_{(Z\rightarrow\tau\tau)/(Z\rightarrow q\bar{q})}$). These estimators are described in reference [2].

Such a method of normalisation is mandatory for the $\gamma\gamma\rightarrow\tau^+\tau^-$ background. First, the rate of such events in the data is very sensitive to the trigger, second the tracks are essentially at very low momentum, in the region of large misidentification, which could change the efficiency of the 2-photon rejection.

The 2-photon background is therefore normalised in two steps. The **PID** is used to tag $\gamma\gamma\rightarrow\tau^+\tau^-$ background among the low energy events (sample A). The acollinearity distribution of the sample A is used to normalise the $\gamma\gamma\rightarrow\tau^+\tau^-$ Monte Carlo to the excess in the data versus the KORALZ $\tau^+\tau^-$ at large acollinearity. The low energy events which are not in sample A are used to normalise the $\gamma\gamma\rightarrow$ e$^+$e$^-$ or $\gamma\gamma\rightarrow\mu^+\mu^-$ Monte Carlo, to the excess in the data versus the KORALZ $\tau^+\tau^-$, at low missing transverse momentum.

3.6 The results

Figure 14 shows the distribution of the electron momentum. A good agreement is observed with the predicted distributions from the $\tau^+\tau^-$ Monte Carlo and the estimated rate of non-tau background.Similarly, figure 15 shows the distribution of the muon momentum. Averaging the results on the 1991-1995 data, the tau lepton branching ratio is :

$$\begin{aligned}\mathcal{B}(\tau^-\rightarrow\nu_\tau e^-\bar{\nu}_e) &= (17.778\pm0.080\pm0.049)\%\ ,\\ \mathcal{B}(\tau^-\rightarrow\nu_\tau\mu^-\bar{\nu}_\mu) &= (17.299\pm0.077\pm0.045)\%\ .\end{aligned}$$

4 Combination of the two analyses

The compatibility between the two sets of results has first to be assessed. For this purpose as well as for the purpose of combination the correlations are investigated. The samples of events have been compared

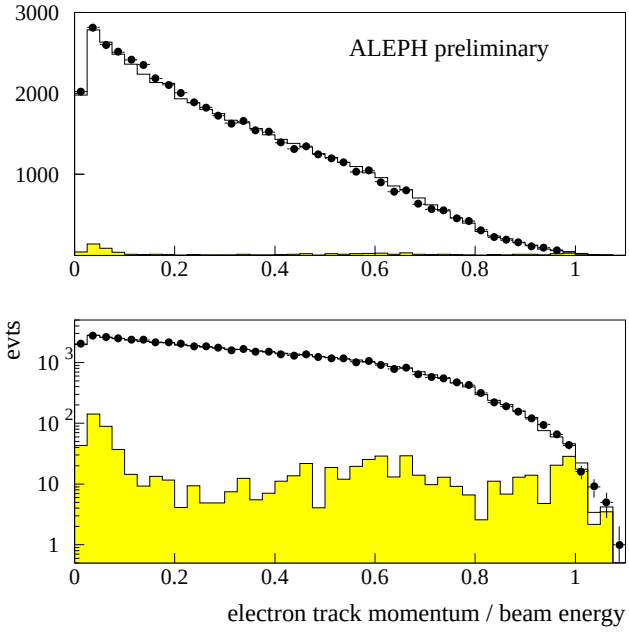

Figure 14: Momentum spectrum for electrons in full LEP 1 data. The Monte Carlo prediction is given by the histogram, with the non-τ background shown in shaded histogram.

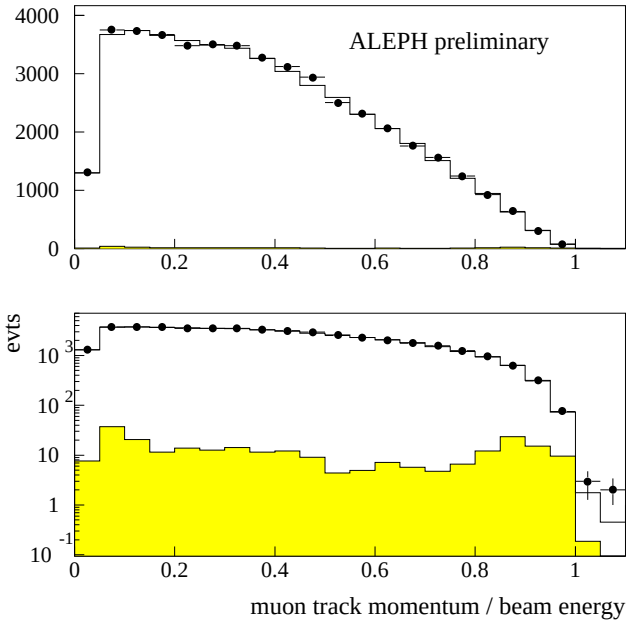

Figure 15: Momentum spectrum for muons in full LEP 1 data. The Monte Carlo prediction is given by the histogram, with the non-τ background shown in shaded histogram.

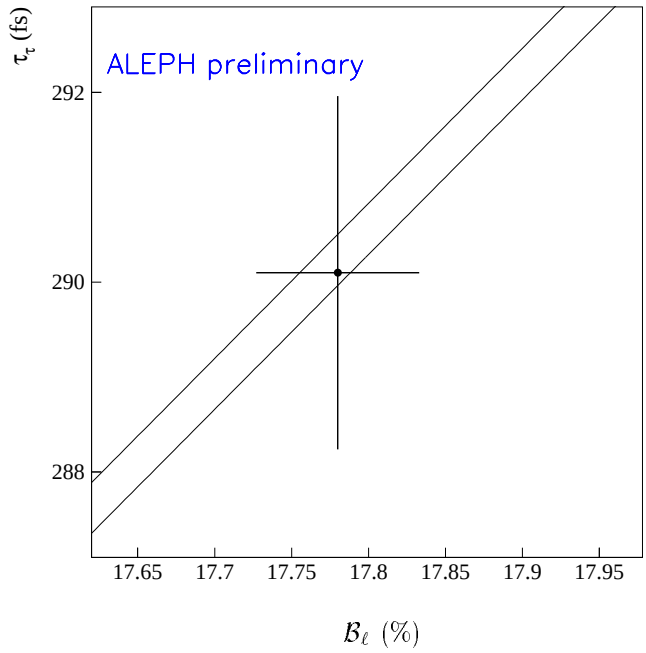

Figure 16: Test of the τ universality with e/μ in the plane $(\tau_\tau, \mathcal{B}_\ell)$, where $\mathcal{B}_\ell$ is $\mathcal{B}\ (\tau \to \ell^{(m_\ell=0)}\,\nu_\ell\,\nu_\tau)$. The frame is defined as a relative range of ± 1 % for each variable. The two straight lines correspond to the prediction of the standard model, assuming universality, with the uncertainty on the tau mass.

and the correlations found to be 0.896 for muons and 0.861 for electrons. The correlated systematics have been identified as being the Monte Carlo statistics for the years 1994 and 1995, the published analysis was done with a Monte Carlo different from the one used in the new analysis, and the particle identification, even though the programs are different the methods use the same information in a quite similar way. The other effects are treated in a very different way, in particular when the new method relies on the measurement of the cross section, the other one computes the branching ratio by identifying a channel as a subsample of the tau sample.

Once all the correlations taken into account, the two measurements of the electronic branching ratio are 0.2 standard deviations away, and the muonic one 0.2. It is then natural to combine them to get the best estimate of the branching ratios. This is straightfoward but for the treatment of the statistical error correlation since one of the methods selects first the tau sample and then the electron and muon channels, when the other one uses the luminosity and the cross section measured elsewhere, but with the same sample.

To do the combination, the statistical error for the second method has been treated as the quadratic sum of two terms. The first one corresponds to the tau sample statistical error, the second to the binomial error of the channel subsample considered in the tau sample. This second part only has been treated as correlated to the first method statistical error.

As the combination is optimised for the total error, the meaningful results are:

$\mathcal{B}_e$ =17.783 $\pm$0.078 % for electrons and $\mathcal{B}_\mu$ =17.290 $\pm$0.076 % for muons. These errors can be approximately separated into a statistical and a systematic uncertainties:

$$\begin{aligned} \mathcal{B}(\tau^- \to \nu_\tau e^- \bar{\nu}_e) &= (17.783 \pm 0.072 \pm 0.032)\,\% \ , \\ \mathcal{B}(\tau^- \to \nu_\tau \mu^- \bar{\nu}_\mu) &= (17.290 \pm 0.069 \pm 0.029)\,\% \ . \end{aligned}$$

This shows that, even at the end of LEP I, the errors are still largely statistics dominated.

4.1 The test of the Standard Model

4.1.1 Test of the μ-e universality

The correlation between the electron and muon measurement is found to be -10.6% in the first method and -4.6% in the second method.

The ratio of the 2 leptonic branching ratios gives :

$$\frac{\mathcal{B}_\mu}{\mathcal{B}_e} = 0.9727 \pm 0.0060 \text{ (stat.)} \pm 0.0016 \text{ (syst.)}$$

in good agreement with the expected value of 0.9726, given the mass of the muon and the tau lepton. This allows to test the lepton universality in the charged current:

$$\frac{g_\mu}{g_e} = 1.0001 \pm 0.0031 \pm 0.0008$$

Where g_ℓ is the leptonic coupling at the W$\ell\bar{\nu}_\ell$ vertex. Assuming e-μ universality in the charged current, we obtain the tau branching ratio to lepton in the massless lepton limit.

$$\mathcal{B}\ (\ \tau \rightarrow \ell^{(m_\ell=0)} \nu_\ell \nu_\tau) = (\ 17.780 \pm 0.046(\text{stat}) \pm 0.026(\text{syst})\ )\%$$

4.1.2 Test of the τ-μ and τ-e universality

Using the rate of $\mu \rightarrow e(\gamma)\nu_e\nu_\mu$ and the tau leptonic branching ratio measured here, the charged leptonic coupling can be tested. The ratio of g_τ to g_μ can be written as a function of the lifetimes, the masses and the tau branching fraction to leptons, with small electroweak and QED corrections[1] yields :

$$\frac{g_\tau}{g_e} = 0.9994 \pm 0.0022(\mathrm{B}_\mu) \pm 0.0017(\tau_\tau) \pm 0.0004(\mathrm{m}_\tau)$$

$$\frac{g_\tau}{g_\mu} = 0.9997 \pm 0.0022(\mathrm{B}_e) \pm 0.0017(\tau_\tau) \pm 0.0004(\mathrm{m}_\tau)$$

and

[1] The parameters used in the test of universality are the following: the tau mass is $1777.05^{+0.29}_{-0.26}$ MeV, the tau lifetime is 290.5 $\pm$ 1.0 fs , the weak correction ΔW = 0.99971 [1] and the QED correction $\Delta\gamma = 1.+8.5\ 10^{-5}$ [1]

$$\frac{g_\tau}{g_{e,\mu}} = 0.9995 \pm 0.0015(\mathrm{B}_\ell) \pm 0.0017(\tau_\tau) \pm 0.0004(\mathrm{m}_\tau)$$

The universality τ-e and τ-μ is verified at 3 per mille, a level similar to e-μ universality. Using the tau branching ratio to massless lepton and the e-μ universality, within the standard model, the tau lifetime can be predicted. It is shown in figure 16, where a good agreement is observed between the predicted and observed tau lifetime.

5 Conclusion

Samples of electron and muon hemispheres have been selected for measuring the probability for taus to decay into electron and muon. The complete LEP I data sample contains about 200000 τ-pair events. Two independent methods have been used. They provide perfectly compatible results which have been therefore combined.

The tau leptonic branching ratios are measured to be (preliminary results):

$$\begin{aligned} \mathcal{B}(\tau^- \to \nu_\tau e^- \bar{\nu}_e) &= (17.783 \pm 0.072 \pm 0.032)\,\% \,, \\ \mathcal{B}(\tau^- \to \nu_\tau \mu^- \bar{\nu}_\mu) &= (17.290 \pm 0.069 \pm 0.029)\,\% \,. \end{aligned}$$

That constitutes the most precise measurement of these branching ratios obtained in a single experiment today.

From these measurements the universality of the charged current couplings to τ, μ and electron is tested at the level of 3 per mille.

References

[1] ALEPH Collaboration, Z. f. Phys. **C70** (1996) 561.

[2] ALEPH Collaboration, Measurement of the tau polarisation at LEP 1, ICHEP98 abst-939 and ALEPH conf 98-037

[3] ALEPH Collaboration, Z. f. Phys. **C70** (1996) 579.

[4] ALEPH Collaboration, Z. f. Phys. **C62** (1994) 539.

[5] ALEPH Collaboration, Measurement of the Z resonance parameters, to be published.

[6] ALEPH Collaboration, Performance of the ALEPH detector at LEP, N.I.M. A360 (1995), 481

[7] H.Anlauf et al, Comp. Phys. Comm. 79 (1994), 466

[8] S.Jadach et al, Comp. Phys. Comm. 76 (1993), 361

[9] I.F. Ginzburg and V.G. Serbo, Phys. Lett. B109 (1982),231

[10] F.A. Berends et al, Nucl. Phys. B304 (1988), 712

[11] E.Tournefier, Mesure du rapport Rℓ avec l'expérience ALEPH à LEP 1,
Thèse Université PARIS-SUD , LAL 98-21

[12] J.M.Hilgart et al, Comput. Physi. Comm. 75 (1993), 191
ALEPH collaboration , CERN-PPE/94-169

[13] S.Narison, Nucl. Phys B40 (1995), 47